Unsymmetrical zinc phthalocyanines containing thiophene and amine groups as donor for bulk heterojunction solar cells

Gülnur KESER KARAOĞLAN[a,*], Öznur DÜLGER KUTLU[a], Ahmet ALTINDAL[b]

[a]Department of Chemistry, Yıldız Technical University, İstanbul, Turkey

[b]Department of Physics, Yıldız Technical University, İstanbul, Turkey

* Corresponding author. E-mail: gkeser@yildiz.edu.tr

ORCIDs:

Ahmet ALTINDAL: https://orcid.org/0000-0002-2185-4094

Gülnur KESER KARAOĞLAN: https://orcid.org/0000-0002-1765-1630

Öznur DÜLGER KUTLU: https://orcid.org/0000-0002-4387-1186

Cite as: Keser Karaoğlan G, Dülger Kutlu Ö, Altındal A. Unsymmetrical zinc phthalocyanines containing thiophene and amine groups as donor for bulk heterojunction solar cells. Turkish Journal of Chemistry. doi: 10.3906/kim-2010-1

Abstract

Photovoltaic technology is an alternative resource for renewable and sustainable energy and low costs organic photovoltaic devices such as bulk-heterojunction solar cells (BHJ) are selective candidates for the effective conversion of solar energy into electricity. Asymmetric phthalocyanines containing electron acceptor and donor groups create high photovoltaic conversion efficiency in dye sensitized solar cells. In this study, a new unsymmetrical zinc phthalocyanine was designed and synthesized including thiophene and amine groups at peripherally positions for BHJ solar cell. The structure of the targeted compound (**4**) was characterized comprehensively by FT-IR, UV–Vis, ^{1}H-NMR and MALDI-TOF MS spectroscopies. The potential of this compound in bulk heterojunction (BHJ) photovoltaic devices as donor was also researched as function of blend ratio (blend ratio was varied from 0.5 to **4**). For this purpose, a series of BHJ devices with the structure of fluorine doped indium tin oxide (FTO)/poly(3,4-ethylenedioxythiophene):poly(styrenesulfonate)/ ZnPc:[6,6]- phenyl-C61- butyric acid methyl ester (PCBM) blend/Al with identical thickness of ZnPc:PCBM layer were fabricated and characterized. Photo current measurements in **4** revealed that the observed photo current maximum is consistent with UV-vis spectra of the compound of **4**. Preliminary studies showed that the blend ratio has critical effect on the BHJ device performance parameters. Photovoltaic conversion efficiency of 6.14% was achieved with **4** based BHJ device

Keywords: Unsymmetrical phthalocyanine; amine; thiophene; bulk heterojunction solar cell; photovoltaic.

1. Introduction

Due to the negative impact on the environmental using fossil fuels, the investigation for renewable energy research has taken its place as an indispensable subject of study worldwide. Therefore, photovoltaic organic solar cells (OSCs) based on organic sources have been the center of rising attention due to their flexibility, light weight, solution processability and as an inexpensive cost photovoltaic energy material [1-3]. The efficiency of photovoltaic organic solar cells is greatly increased by adding of the bulk-heterojunction (BHJ) term [4-8] being an active fragment where electron acceptor and donor materials are blended in a solution and placed into a thin film sandwiched between two electrodes. Recently, huge progresses are being accomplished in development the power conversion capacity (PCE) of organic Bulk heterojunction solar cells. BHJ solar cells, based on polymer / fullerene combination, have attracted a great deal due to power conversion efficiency of over 10% [9-13]. Higher power conversion efficiencies are now obtained using low-band gap polymers that allow the collection of a wider segment of the solar spectrum [14,15].

Material innovation is an important factor that determines the efficiency of organic solar cells. Some polymer types have been preferred as electron- donor in solar cell studies [16]. Fullerenes and their derivatives which have been widely preferred as electron acceptor materials in OSCs and the poly(3-hexylthiophene-2,5-diyl) (P3HT) as the electron donor are among the most widely used materials for industrialization in BHJ solar cell technology [17-18]. [6,6]-phenyl-C61- butyric acid methyl ester (PCBM), one of these fullerene derivatives, has fabulous photovoltaic features [19].

Phthalocyanines (Pcs), which are decent p-type semiconductors, offer active redox chemistry that can be modulated as a function of the periferal substitute groups and / or

the central metal in the aromatic space of the pc ring. Consequently, when photoexcited, Pcs are capable of acting either as lectron-acceptors when linked to donor systems such as polythiophenes [20], or electron-donors when they are connected to suitable electron-acceptor groups such as fullerenes [21]. Although significant progress has been made for high-performance BHJ solar cells with P3HT, it has some disadvantages, such as a restricted absorption wavelength [22]; hence, there is an obligation to improve new donor materials having larger absorption in the red region. For this purpose, Pcs are commonly used donor compounds in solar cells. All these properties make these structures worthy photoactive materials. Normally, P3HT molecule absorbs light from 400 to 600 nm, but it is connected to a Pc molecule absorbs light at wavelengths between 600 and 700 nm to the active layer will lead to a broadening of the absorption range. Lately, the clear contribution of the Pc around 700 nm to the photocurrent has been proved by Torres et al [23]. There are many studies on thiophene derivatives as π-conjugated organic molecules because of their structural planarity permits strong electronic conjugation within the structure as well as their stability and well known synthetic chemistry. For these reasons, attachment of these thienyl motions at the Pc ring as peripherally positions might result in the enlargement and improvement of the π-conjugation systems [24,25].

We report herein on the synthesis of unsymmetrical tetra substituted zinc phthalocyanines linked thiophene and amine groups at the peripheral positions and the use of electron donating novel phthalocyanines obtained in BHJ devices as an alternative to P3HT material has yielded successful results. The thiophene groups were chosen to provide the electron-releasing effect for the electronic properties of phthalocyanines. The combination of the sulfur atom in thiophene and amine groups as

substituent in newly designed unsymmetrical zinc phthalocyanine has significantly improved performance of BHJ.

2. Experimental design

All information about the used materials, equipment, synthesis, improved performance of BHJ and photovoltaic behaviours were shown in the "Supplementary Information" [26,30].

3. Results and Discussion

3.1 Synthesis and characterization

Today, asymmetric metal phthalocyanines (MPcs) have been the focus of attention in order to fine-tune the properties of these complexes because symmetrical MPcs do not always meet the requirement for developing large technology applications [31]. The new unsymmetrical phthalocyanine including thiophene groups (**4**) was synthesized via step by step. After tetra-nitro-ZnPc derivative (**1**) was synthesized, tetra-amine-ZnPc (**2**) was synthesized by the reduction of tetra-nitro-ZnPc in the medium of hydrazine hydrate and 10% Pd/C as the catalyst [26]. Finally **4** was obtained with the statistical reaction of (**2** and **3**) affording in principle a mixture of two A_2B_2 type unsymmetrical zinc phthalocyanines complexes (Figure 1).

After chromatographic separation unique spot was obtained for complex **4**. To approve chemical structure of the new asymmetric Pc complex (**4**) spectroscopic methods were used such as UV–Vis, FT-IR, ^{1}H-NMR and MALDI-TOF MS spectroscopies. Most of phthalocyanines especially unsubstituted ones have low solubility in many organic solvents; however substation of suitable functional groups on the Pc ring improve the

solubility such as thiophene, alkyl, phenoxy and alkoxy groups. Pc (**4**) obtained by binding thiophene groups to tetra amine Pc (**2**) showed good solubility like Pc (**2**) in many common solvents such as THF, $CHCl_3$, DMF and DMSO.

For unsymmetrical zinc phthalocyanine derivation (**4**), the characteristic –N = C stretch at 1679 cm^{-1} was appeared in the FTIR spectrum, indicative of expected structure. The characteristics vibrations corresponding to amine groups (-NH_2) were observed at 3343, 3231, 1609 cm^{-1} (for **4**). Aromatic CH stretching at 3064 cm^{-1} was observed for the complex. Stretching vibration of thiophene rings in Pc complex **4** was also detected at 833 cm^{-1}.

The UV–Vis spectra of the Pcs **1**, **2** and **4** are given in Figure 2 in THF. In these spectra, two bands were observed: Soret or B band (350–352 nm) in the UV region and Q band (679–707 nm) in the visible region [32]. When the UV-Vis spectra of compounds **1** and **2** are compared, the shift observed between the Q band absorption peaks is caused by the reduction of the -NO_2 groups in the peripheral positions to the electron donor -NH_2 groups. Spectra of **2** and **4** in THF have intense Q bands at 707 and 690 nm due to a single π- π^* transition with shoulders at 635 and 626 nm, respectively. 9 nm blue shifting was observed for asymmetric Pc compare to amine Pc due to binding thiophene groups on peripherally positions However, the Soret (B) bands are observed at similar wavelengths as 350 and 352 nm, respectively (Table 1).

The newly synthesized Pc **4** was characterized by ^{1}H-NMR spectrum which was observed to be in good correlation with its own structure. **4** showed the phthalocyanine skeleton protons and thiophene protons as multiples between 9.06 and 6.99 ppm as expected. The -NH_2 protons at 4.38 ppm as singlet for 4 protons.

Also unsymmetrical Pc **4** was characterized by MALDI-TOF MS where molecular ion peak atm/z: 687.437 $[M-2NH_2 -C_9H_6NS_2-C_4H_3S+2H]^+$, 1013.27 $[M+Na+2H]^+$., clearly indicates the formation of desired products as A_2B_2 types.

In the Figure 1, it is seen that the spectral data of the newly synthesized compounds confirm the proposed structures.

3.2 Photovoltaic characterization

It is well known that the surface morphology of the blend film are also importance for the photovoltaic performance of the phtalocyanine based bulk heterojunction solar cells. In order to clarify the effect of the surface morphology of the blend film on the photovoltaic performance, the surface morphology of the blend film were analyzed by atomic force microscopy. The AFM image analysis was performed with commercial programmes associated with XEI and XEP software application to determine the surface roughness characterized by the Root–Mean– Square (RMS) parameter. As a represantative results, Figure 3 (a) and (b) shows the AFM surface topography of the blend films of **4.0:**1.0 and **2.5:**1.0, respectively. It is clear that the films morphology were considerably affected by the **4** ratio. The film with **4.0**:1.0 blend ratio exhibited higher surface roughness, while films with **2.5**:1.0 blend ratio have displayed lower root mean square (rms) roughness. From the close analysis of the AFM images, the surface roughness was determined and was found to be 60 and 45 nm for the film with **4.0**:1.0 and **2.5**:1.0 blend ratio, respectively.

Before the photo voltaic characterization, the conductivity of the PEDOT:PSS film and the photocurrent vs. incident light wavelength measurements were carried out. Our results indicated that the conductivity of the PEDOT:PSS film was about 0.35 S/cm.

The variation of the photo current with the incident light wavelength is presented in Figure 4 for the film of **4**. It should be mentioen here that maximum photoconductivity was obdserved with **4** based film for all incident light wavelength. As is clear, the photo current increases with the increase in incident light wavelength, goes through a maximum at a certain wavelength and then decreases.

Maximum photocurrent was observed at about 690 nm which is consistent with UV-Vis spectra of the compound of **4**. The wavelength dependence of the monitored photo current expresses that vigorously absorbed photons are mainly responsible for free carrier production and therefore photocurrent.

In order to evaluate the photovoltaic performance of **4** in BHJ solar cells as donor and the effect of the blend ratio on the main performance parameters a series of BHJ devices with FTO/PEDOT:PSS/**4**:PCBM blend/Al structure were fabricated and characterized. During the fabrication and characterization studies, the ratio of PCBM was fixed at 1 and the ratio of donor (**4)** was varied from 0.5 to 4.0 because of its well known critical impact on the device performance [33]. Current density-voltage (J-V) characteristics obtained with the FTO/PEDOT:PSS/**4**:PCBM blend/Al structure of BHJ solar cells devices with various blend ratio under AM 1.5 G illumination is shown in Figure 5 and evaluated performance parameters tabulated in Table 2. At first glance, it is obvious that all the devices fabricated exhibit rectifying behavior with various rectification ratios depending on the blend ratio. It is also clear that the photovoltaic performance parameters of the devices are modulated by the blend ratio of **4**: PCBM. As usual, photovoltaic conversion efficiency of a solar cell which is defined as

$$\eta = \frac{P_m}{P_{in}} \qquad (1)$$

where P_{in} is the power of incident light, P_m is maximum power output of the cell which is defined as

$$P_m = J_{SC} \times V_{OC} \times FF \quad (2)$$

in the following equation; FF expressed as the filling factor is defined as the maximum power output of the solar cell per unit area divided by the product of V_{OC} and J_{SC}.

$$FF = \frac{J_m \times V_m}{J_{sc} \times V_{oc}} \quad (3)$$

where J_m and V_m are the current density and voltage at which the cell delivers the maximum power density. Interestingly, it was observed that the open circuit voltage (V_{OC}) of the devices increases with the increase of **4** ratio in the blend solution, when the blend ratio of **4**:PCBM reached **2.5**:1 the best **4**:PCBM based cell was realized as shown in Figure 5, and then V_{OC} decreases with further increase of **4** ratio (see Table 2). From the close investigation of the Table 2, it will be clear that the performance of the devices strongly depend on the blend ratio, photovoltaic conversion efficiency of the device varies between 3.32% for **4.0**:1.0 blend ratio and 6.14% for **2.5**:1.0 blend ratio. The V_{OC}, J_{SC}, FF, and efficiency of the champion device were 0.95 V, 11.70 mA/cm^2, 0.55 and 6.14 %, respectively. To our knowledge, these values are the highest reported for phthalocyanine based bulk heterojunction solar cells. In order to be sure that the dependence of the observed open circuit voltage on blend ratio is repeatable, the J-V measurements were repeated for another set of the devices from the same batch of the devices and these measurements verified that the observed dependence of open circuit voltage on the blend ratio are reproducible, except for a small shift in its value. It is well known that P3HT and PCBM are frequently preferred donor and acceptor substances in BHJ devices. Previous works on the BHJ devices made from P3HT: PCBM blends with

various blend ratios have indicated that the photo voltaic performances of these devices strongly depend on the blend ratio [34-36].

The energetic disturbance of organic semiconductors, compared to their crystalline inorganic counterparts, causes the intramolecular and intermolecular interactions in a morphologically diverse film to expand the distribution of electronic states and is significantly affected by structural properties. Regardless of the functional shape (Gaussian or an exponential function-or a combination of these two) of density of states, increased broadening of the density of states invariably pushes tail states further into the band gap, and this leads to strong correlations between disorder and voltage losses in solar cells [37]. More recent reports on planar heterojunction [38] as well as bulk heterojunction solar cells [39-41] have shown that the open circuit voltage is strongly dependent on the difference between the highest occupied molecular orbital (HOMO) of the donor and the lowest unoccupied molecular orbital (LUMO) of the acceptor materials. It is proposed that the nanoscale morphology of the two components (donor/acceptor) in the photoactive layer and the efficient separation of charges at the donor– acceptor interface in bilayer planar and non-planar metal Pc/ C60 solar cells are also crucial in determining the V_{OC} value. Relationship between energetic disorder and open-circuit voltage in bulk heterojunction organic solar cells has been investigated by Blakesley et al [42]. They were reported that the open circuit voltage associated with the charge-carrier recombination rates, donor-acceptor energy gap, contact work functions, illumination intensity and the amount of energetic disorder. The complex factors leading open circuit voltage losses through energetic disorder in BHJ solar cells have been investigated by Nguyen et al [43]. It was reported that disorders contribute as much as 0.2 V of V_{OC} loss. A reasonable explanation for the observed ratio dependence

has been given by the eutectic phase behavior of donor and acceptor blends and suggested that morphology at the optimum composition ratio is slightly hypoeutectic [44,45].

To access efficient exciton dissociation in BHJ devices, the randomly oriented donor acceptor interfaces are employed and the performance of the devices are determined by the morphology of the donor-acceptor interface [46,47], the molecular orientation and aggregation behavior [48,49]. On the other hand, it is well known that interfacial energetic, which involves tightly bounded singlet excitonic states and loosely bounded charge transfer states, have direct impacts on open circuit voltage of the BHJ devices [47,50,51] It was reported previously that the upper limit of the open circuit voltage is determined by the loosely bounded charge transfer states and their disordered effect [52-54]. The obtained J−V characteristics for devices with a fixed donor material and different fullerene based acceptor materials indicated that, as the acceptor with higher lowest unoccupied molecular orbital level is employed, the open circuit voltage becomes larger due to the increased effective band gap [55].

Metal-Insulator-Metal (MIM) model is widely used to interpret and analyze the obtained open circuit voltage data. The MIM model assumes that the upper limit of the V_{OC} is determined by the work function difference of the anode and cathode materials. Figure 5 clearly shows that, if the origin of the V_{OC} is due to the work function difference all the devices should yield a V_{OC} values of 0.47 (Work functions of FTO and Al is 4.80 and 4.33 eV, respectively), the MIM model can not be applied to our devices. More recently, many theoretical and experimental studies on BHJ have shown that the V_{OC} is independent of the choice of cathode materials and depends on various factors including, energetic disorder in active layer, donor-acceptor energy gap, and rate of

charge recombination [56-58]. Effects of blend composition on the morphology of Si-PCPDTBT: PC71BM based bulk heterojunction organic solar cells have been studied by Lin et al. [59] and it was reported that the exciton dissociation efficiency is highly dependent on the content of blend. For further understanding of the composition dependence of the performance of a BHJ device, the structural evolution during blend crystallization for P3HT:PCBM blends were investigated by Barrena et. al. [60]. They reported that donor:acceptor blends with ratios of 1.0:0.5, 1.0:0.8, and 1.0:2.0 exhibit differing microstructure during solidification. Therefore, the observed blend ratio dependence for open circuit voltage can be related to a differing nature of the microstructure of the blend films.

High level blend ratio of **4** give rise to more disordered film formation because of the high aggregation tendency of phthalocyanine molecule. Increased disordering in active layer leads to a decrease in exciton diffusion length, which destabilizes the charge separated states. Destabilization of the charge separated states leads to an increase in charge recombination rate which could result in a decrease in V_{OC}. The observed trend for short circuit current density supports this conclusion. By a close analysis of the Figure 5, it becomes clear that the short circuit current density follows the same trend with VOC, it increases with the increase of **4** ratio in the blend solution and reaches a maximum when the blend ratio of **4**:PCBM reached **2.5**:1. As well known short circuit current density is another key parameter for a solar cell, which is determined by the product of photoinduced charges and their mobility. It was reported before by Gulbinas et al. [58] that the short circuit current density in a BHJ solar cell device is determined by the charge separation into free carriers which is strongly influenced by the blend ratio. It was also reported that the charge separation is efficient in PCBM rich blends,

suggesting that high mobility of one type of carriers is essential for efficient charge separation, and morphology optimization doubles the charge pair separation efficiency and the short circuit current density. It can be again concluded that the structural evaluation during blend crystallization for **4**:PCBM blends play crucial role in defining the basic performance parameters of a BHJ device.

Conclusion

Unsymmetrical zinc phthalocyanine (**4**) bearing thiophene and amine groups as donor was successfully synthesized as confirmed by FT-IR, UV-Vis, ^{1}H-NMR and MALDI-TOF MS. Bulk heterojunction solar cell devices using blended **4**:PCBM with eight different donors: acceptor ratios have been fabricated and characterized. Our preliminary results showed that the entire device fabricated exhibited photovoltaic character. It was also found that the ratio of donor: acceptor has a significant effect on the photovoltaic behavior of the devices. Photovoltaic conversion efficiency of 6.14% was achieved with **4** based device.

References

1. Li N, Baran D, Spyropoulos GD, Zhang H, Berny S et al. Environmentally printing efficient organic tandem solar cells with high fill factors: a guideline towards 20% power conversion efficiency. Advanced Energy Materials 2014; 4 (11): 1-7. doi: 10.1002/aenm.201400084

2. Rossander LH, Zawacka NK, Dam HF, Krebs FC, Andreasen J. In situ monitoring of structure formation in the active layer of polymer solar cells during roll-to-roll coating. AIP Advances 2014; 4 (8): 1-8. doi: 10.1063/1.4892526

3. Scharber MC, Sariciftci NS. Efficiency of bulk-heterojunction organic solar cells. Progress in Polymer Science 2013; 38 (12): 1929-1940. doi: 10.1016/j.progpolymsci.2013.05.001

4. Irwin MD, Buchholz B, Hains AW, Chang RPH, Marks TJ. p-Type semiconducting nickel oxide as an efficiency-enhancing anode interfacial layer in polymer bulk-heterojunction solar cells. Proceedings of the National Academy of Sciences 2008; 105 (8): 2783-2787. doi: 10.1073/pnas.0711990105

5. Itoh E, Maruyama Y, Fukuda K. Photovoltaic properties of bulk-heterojunction organic solar cell with ultrathin titanium oxide nanosheet as electron selective layer. Japanese Journal of Applied Physics 2013; 52 (4). doi: 04CK05. 10.7567/JJAP.52.04CK05

6. Mihailetchi VD, Koster LJA, Blom PWM, Melzer C, De Boer B et al. Compositional dependence of the performance of poly(p-phenylene vinylene):methanofullerene bulk-heterojunction solar cells. Advanced Energy Materials 2005; 15 (5), 795-801. doi: 10.1002/adfm.200400345

7. Ren BY, Ou CJ, Zhang C, Chang YZ, Yi MD et al. Diarylfluorene-modified fulleropyrrolidine acceptors to tune aggregate morphology for solution-processable polymer/fullerene bulk-heterojunction solar cells. The Journal of Physical Chemistry C 2012; 116 (16): 8881- 8887. doi: 10.1021/jp212254g

8. Scharber MC, Wuhlbacher D, Koppe M., Denk P, Waldauf C et al. Design rules for donors in bulk-heterojunction solar cells—towards 10 % energy-conversion efficiency. Advanced Materials 2006; 18 (6): 789–794. doi: 10.1002/adma.200501717

9. Liu Y, Zhao J, Li Z, Mu C, Ma W et al. Aggregation and morphology control enables multiple cases of high-efficiency polymer solar cells. Nature Communications 2014, 5: 1-8. doi: 10.1038/ncomms6293

10. Brabec CJ, S Gowrisanker, Halls JJM, Laird D, Jia SJ et al. Polymer-fullerene bulk-heterojunction solar cells. Advanced Materials 2010; 22 (34): 3839–3856. doi: 10.1002/adma.200903697

11. Li G, Zhu R, Yang Y. Polymer solar cells. Nature Photon 2012; 6: 153–161. doi: 10.1038/nphoton.2012.11

12. He ZC, Zhong CM, Su SJ, Xu M, Wu HB et al. Enhanced power-conversion efficiency in polymer solar cells using an inverted device structure. Nature Photonics 2012; 6 (9): 591–595. doi: 10.1038/nphoton.2012.190

13. Darling SB, You F. The case for organic photovoltaics. Royal Society of Chemistry Advances 2013; 3 (39): 17633–17648. Doi: 10.1039/C3RA42123F

14. JB You, Dou L, Yoshimura K, Kato T, Ohya K et al. A polymer tandem solar cell with 10.6% power conversion efficiency. Nature Communications 2013; 4: 1-10. doi: 10.1038/ncomms2411

15. Liang Y, Yu L. A new class of semiconducting polymers for bulk heterojunction solar cells with exceptionally high performance. Accounts of Chemical Research 2010; 43 (9): 1227–1236. doi: 10.1021/ar1000296

16. Dennler G, Scharber MC, Brabec CJ. Polymer-fullerene bulk-heterojunction solar cells. Advanced Materials 2009; 21 (13): 1323–1338. doi: 10.1002/adma.200801283

17. Dang MT, Hirsch L, Wantz G. P3HT:PCBM, Best seller in polymer photovoltaic research. Advanced Materials 2011; 23 (31): 3597–3602. doi: 10.1002/adma.201100792

18. Patil Y, Misra R, Singhal R, Sharma GD. Ferrocene-diketopyrrolopyrrole based non-fullerene acceptors for bulk heterojunction polymer solar cells. Journal of Materials Chemistry A 2017; 5: 13625-13633. doi: 10.1039/C7TA03322B

19. Choy WCH. Organic Solar Cells. London ; New York: Springer-Verlag, 2013.

20. Abdullah SM, Ahmad Z, Aziz F, Sulaiman K et al. Investigation of VOPcPhO as an acceptor material for bulk heterojunction solar cells. Organic Electronics 2012; 13(11): 2532–2537. doi: 10.1016/j.orgel.2012.07.030

21. Sánchez-Díaz A, Pacios R, Muñecas U, Torres T, Palomares E. Charge transfer reactions in near IR absorbing small molecule solution processed organic bulk-heterojunction solar. Organic Electronics 2011; 12 (2): 329–335. doi: 10.1016/j.orgel.2010.11.014

22. Smestad GP, Krebs FC, Lampert CM, Granqvist CG, Chopra KL et al. Reporting solar cell efficiencies in solar energy materials and solar cells. Solar Energy Materials and Solar Cells 2008; 92 (4): 371–373. doi: 10.1016/j.solmat.2008.01.003

23. Campo BJ, Duchateau J, Ganivet CR, Ballesteros B, Gilot J et al. Broadening the absorption of conjugated polymers by “click” functionalization with phthalocyanines. Dalton Transactions 2011; 40 (15): 3979–3988. doi: 10.1039/C0DT01348J

24. Roncali J. Conjugated poly(thiophenes): synthesis, functionalization, and applications. Chemical Reviews 1992; 92 (4): 711-738. doi: 10.1021/cr00012a009

25. Muto T, Temma T, Kimura M, Hanabusa K, Shirai H. Elongation of the π-System of phthalocyanines by introduction of thienyl substituents at the peripheral β positions. synthesis and characterization. The Journal of Organic Chemistry 2001; 66 (18): 6109-6115. doi: 10.1021/jo010384r

26. Keser Karaoglan G, Gümrükçü G, Koca A, Gül A, Avcıata U. Synthesis and characterization of novel soluble phthalocyanines with fused conjugated unsaturated groups. Dyes Pigments 2011; 90 (1): 11-20. doi: 10.1016/j.dyepig.2010.10.002

27. Popović D, Ata I, Krantz J, Lucas S, Lindén M et al. Preparation of efficient oligomer-based bulk-heterojunction solar cells from eco-friendly solvents. Journal of Materials Chemistry C 2017; 5 (38): 9920-9928. doi: 10.1039/C7TC02131C

28. Chen X, Liu X, Burgers MA, Huang Y, Bazan GC. Green-solvent-processed molecular solar cells. Angewandte Chemie International Edition 2014; 53 (52): 14378–14381. doi: 10.1002/anie.201409208

29. Farahat ME, Tsao CS, Huang YC, Chang SH. Budiawan W et al. Toward environmentally compatible molecular solar cells processed from halogen-free solvents. Journal of Materials Chemistry A 2016; 4: 7341–7351. doi: 10.1039/C6TA01368F

30. Xiao L, Liu C, Gao K, Yan Y, Peng J et al. Highly efficient small molecule solar cells fabricated with non-halogenated solvents. Royal Society of Chemistry 2015; 5 (112): 92312–92317. doi: 10.1039/C5RA19054A

31. Goktug O, Soganci T, Ak M, Sener MK. Efficient synthesis of EDOT modified ABBB-type unsymmetrical zinc phthalocyanine: optoelectrochromic and glucose sensing properties of its copolymerized film. New Journal of Chemistry 2017; 41 (23): 14080-14087. doi: 10.1039/C7NJ03250A

32. Ceylan N, Gümrükçü G, Keser Karaoglan G, Gül A. Synthesis, characterization, fluorescence spectra and energy transfer properties of a novel unsymmetrical zinc phthalocyanine with peripherally coordinated Ru(II) complex Synthetic Metals 2015; 206: 55-60. doi: 10.1016/j.synthmet.2015.05.013

33. Powroźnik P, Krzywiecki M, Grządziel L, Jakubik W. Study of sensing mechanisms in nerve agent sensors based on phthalocyanine-palladium structures. Procedia Engineering 2016; 168: 586–589. doi: 10.1016/j.proeng.2016.11.220

34. Li G, Shrotriya V, Huang J, Yao Y, Moriarty T et al. High-efficiency solution processable polymer photovoltaic cells by self-organization of polymer blends. Nature Materials 2005; 4 (11): 864-868. doi: 10.1038/nmat1500

35. Kadem B, Hassan A. The effect of fullerene derivatives ratio on P3HT-based organic solar cells. Energy Procedia 2015; 74: 439-445. doi: 10.1016/j.egypro.2015.07.647

36. Ma W, Yang C, Gong X, Lee K, Heeger AJ. Thermally stable, efficient polymer solar cells with nanoscale control of the interpenetrating network morphology. Advanced Functional Materials 2005; 15 (10): 1617-1622. doi: 10.1002/adfm.200500211

37. Lange I, Kniepert J, Pingel P, Dumsch I, Allard S et al. Correlation between the open circuit voltage and the energetics of organic bulk heterojunction solar cells. Journal Of Physical Chemistry Letters 2013; 4 (22): 3865−3871. doi: 10.1021/jz401971e

38. Rand BP, Burk DP, Forrest SR. Offset energies at organic semiconductor heterojunctions and their influence on the open-circuit voltage of thin-film solar cells. Physical Review B 2007; 75 (11): 115327. doi: 10.1103/PhysRevB.75.115327

39. Scharber MC, Wuhlbacher D, Koppe M, Denk P, Waldauf C et al. Design rules for donors in bulk-heterojunction solar cells - Towards 10 % energy-conversion efficiency. Advanced Materials 2006; 18 (6): 789-794. doi: 10.1002/adma.200501717

40. Mihailetchi VD, Blom PWM, Hummelen JC, Rispens MT. Cathode dependence of the open-circuit voltage of polymer: fullerene bulk heterojunction solar cells. Journal of Applied Physics 2003; 94 (10): 6849-6854. doi: 10.1063/1.1620683

41. Altun S, Odabaş Z, Altındal A, Özkaya AR. Coumarin-substituted manganese phthalocyanines: synthesis, characterization, photovoltaic behaviour, spectral and electrochemical properties. Dalton Transactions 2014; 43 (21): 7987–7997. doi: 10.1039/c4dt00482e

42. Blakesley JC, Neher D. Relationship between energetic disorder and open-circuit voltage in bulk heterojunction organic solar cells. Physical Review B 2011; 84 (7): 075210. doi: 10.1103/PhysRevB.84.075210

43. Collins SD, Proctor CM, Ran NA, Nguyen TQ. Understanding open-circuit voltage loss through the density of states in organic bulk heterojunction solar cells. Advanced Energy Materials 2016; 6 (4): 1-11. doi: 10.1002/aenm.201501721

44. Müller C, Ferenczi TAM, Campoy-Quiles M, Frost JM, Bradley DDC et al. Binary organic photovoltaic blends: A simple rationale for optimum compositions. Advanced Materials 2008; 20 (18): 3510–3515. doi: 10.1002/adma.200800963

45. Baumann A, Lorrmann J, Deibel C, Dyakonov V. Bipolar charge transport in poly(3-hexyl thiophene)/methanofullerene blends: A ratio dependent study. Applied Physics Letters 2008; 93 (25): 252104–252106. doi: 10.1063/1.3055608

46. Szarko JM, Rolczynski BS, Lou SJ, Xu T, Strzalka J et al. Photovoltaic Function and Exciton/Charge Transfer Dynamics in a Highly Efficient Semiconducting Copolymer. Advanced Functional Materials 2014; 24 (1): 10-26. doi: 10.1002/adfm.201301820

47. Nuzzo DD, Koster LJA, Gevaerts VS, Meskers SCJ, Janssen RAJ. The role of photon energy in free charge generation in bulk heterojunction solar cells. Advanced Energy Materials 2014; 4 (18): 1400416. doi: 10.1002/aenm.201400416

48. Chen XK, Ravva MK, Li H, Ryno SM, Bredas JL. Effect of molecular packing and charge delocalization on the nonradiative recombination of charge-transfer states in organic solar cells. Advanced Energy Materials 2016; 6 (24): 1601325. doi: 10.1002/aenm.201601325

49. Ryno SM, Ravva MK, Chen X, Li H, Breda JL. Molecular understanding of fullerene – electron donor interactions in organic solar cells. Advanced Energy Materials 2017; 7 (10): 1601370. doi: 10.1002/aenm.201601370

50. Arndt AP, Gerhard M, Quintilla A, Howard IA, Koch M et al. Time-resolved charge-transfer state emission in organic solar cells: temperature and blend composition dependences of interfacial traps. The Journal of Physical Chemistry C 2015; 119 (24): 13516-13523. doi: 10.1021/acs.jpcc.5b03507

51. Grancini G, Maiuri M, Fazzi D, Petrozza A, Egelhaaf HJ et al. Hot exciton dissociation in polymer solar cells. Nature Materials 2013; 12: 29-33. doi: 10.1038/NMAT3502

52. Collins SD, Proctor CM, Ran NA, Nguyen TQ. Understanding open□circuit voltage loss through the density of states in organic bulk heterojunction solar cells. Advanced Energy Materials 2016; 6 (4): 1501721. doi: 10.1002/aenm.201501721

53. Zou Y, Holmes RJ. Correlation between the open-circuit voltage and charge transfer state energy in organic photovoltaic cells. ACS Applied Materials and Interfaces 2015; 7 (33): 18306-18311. doi: 10.1021/acsami.5b03656

54. Guan Z, Li HW, Cheng Y, Yang Q, Lo MF et al. Charge-transfer state energy and its relationship with open-circuit voltage in an organic photovoltaic device. The Journal of Physical Chemistry C 2016; 120 (26): 14059-14068. doi: 10.1021/acs.jpcc.6b02375

55. Hoke ET, Vandewal K, Bartelt JA, Mateker WR, Douglas JD et al. Recombination in polymer:fullerene solar cells with open-circuit voltages approaching and exceeding 1.0 V. Advanced Energy Materials 2013; 3 (2): 220-230. doi: 10.1002/aenm.201200474

56. Brabec CJ, Cravino A, Meissner D, Sariciftci NS, Fromherz T et al. The influence of materials work function on the open circuit voltage of plastic solar cells. Thin Solid Films 2002; 403-404: 368-372. doi: 10.1016/S0040-6090(01)01586-3

57. Blakesley JC, Neher D. Relationship between energetic disorder and open-circuit voltage in bulk heterojunction organic solar cells. Physical Review B 2011; 84 (7): 075210. doi: 10.1103/PhysRevB.84.075210

58. Pranculis V, Ruseckas A, Vithanage DA, Hedley GJ, Samuel IDW et al. Influence of blend ratio and processing additive on free carrier yield and mobility in PTB7:PC71BM photovoltaic solar cells. The Journal of Physical Chemistry C 2016; 120 (18): 9588−9594. doi: 10.1021/acs.jpcc.6b01658

59. Lin R, Wright M, Puthen-Veettil B, Wen X, Tayebjee MJY et al. Effects of blend composition on the morphology of Si-PCPDTBT:PC71BM bulk heterojunction organic solar cells. Physica Status Solidi A-Applications And Materials Science 2015; 212 (9), 1931–1940. doi: 10.1002/pssa.201532009

60. Sanyal M, Schmidt-Hansberg B, Klein MFG, Munuera C, Vorobiev A et al. Effect of photovoltaic polymer/fullerene blend composition ratio on microstructure evolution during film solidification investigated in real time by x-ray diffraction. Macromolecules, 2011; 44 (10): 3795–800. doi: 10.1021/ma2000338

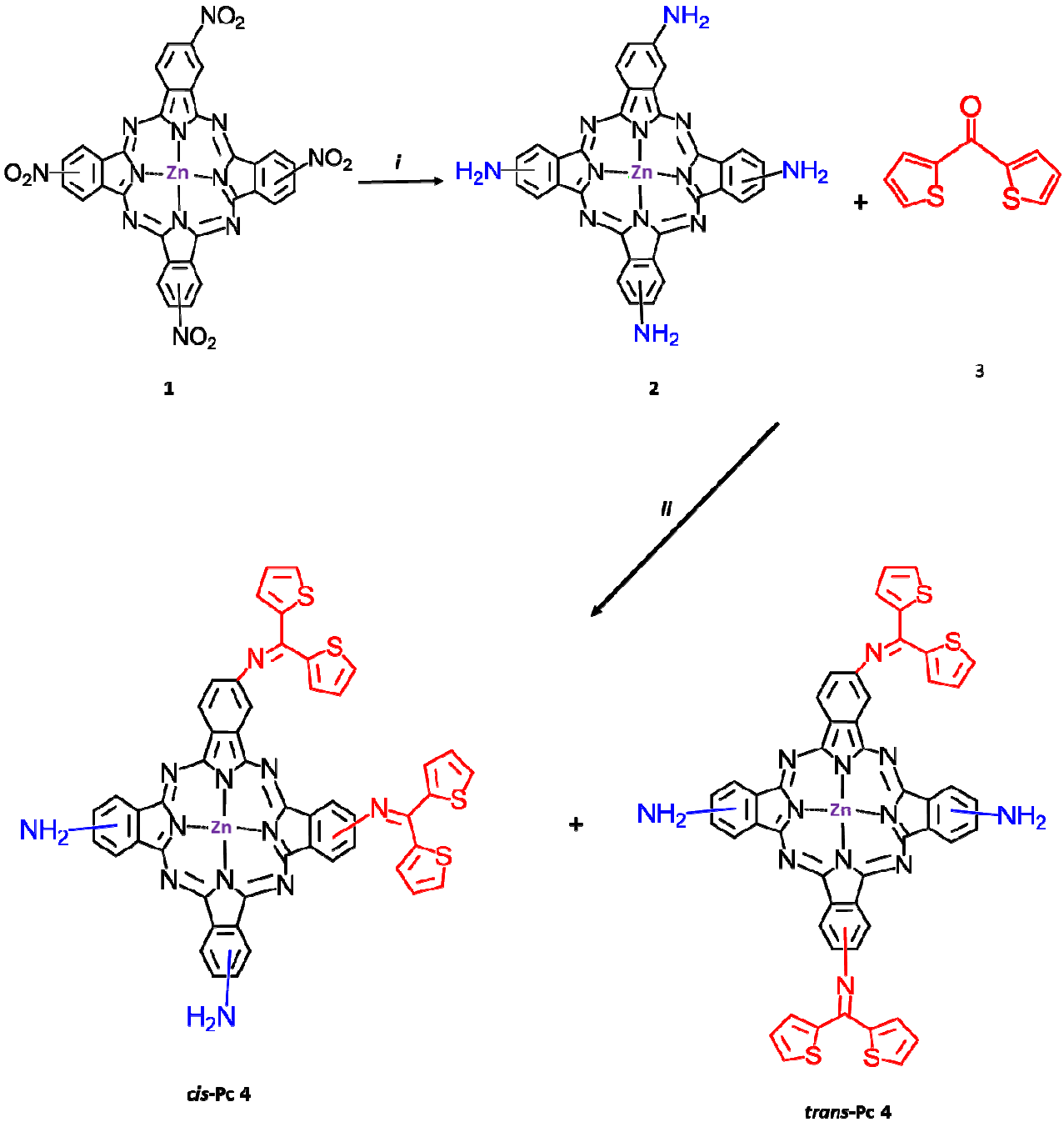

1 **2** **3**

***cis*-Pc 4** ***trans*-Pc 4**

Figure 1. Synthetic route of Pc **4**: (*i*) Pd/C, hydrazine hydrate, 1,4-dioxane; (*ii*) dry DMF, *p*-TsOH·H_2O, 48 h, reflux.

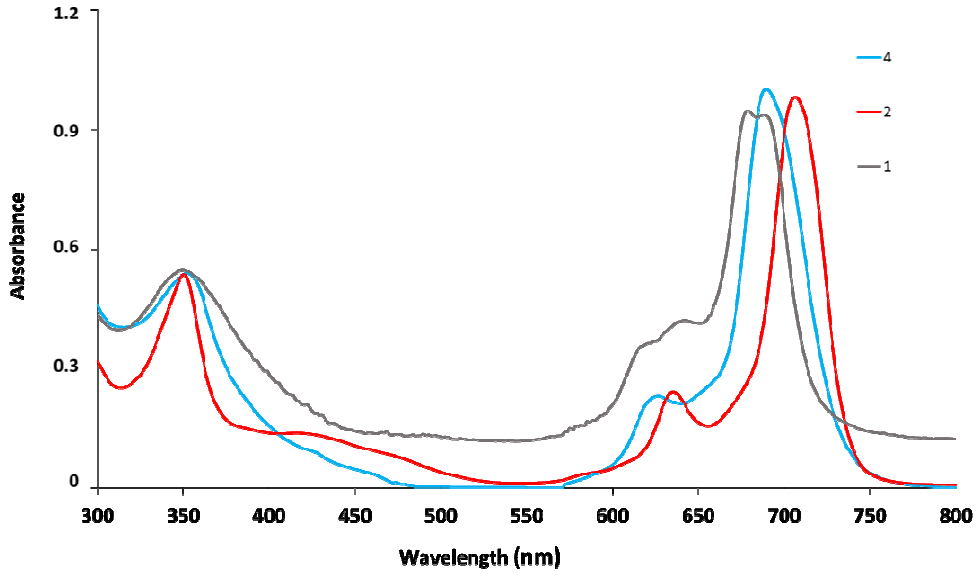

Figure 2. UV-Vis absorption spectra of complex **1**, **2** and **4** in THF (1.0×10^{-5} M)

Table 1

UV-Vis data for zinc phthalocyanine complexes (**1**, **2** and **4**) in THF.

Complex	λ_{max}, nm (log ε, *L mol*$^{-1}$ *cm*$^{-1}$)				
1	350 (4.73)	617[a] (4.55)	639[a] (4.62)	679 (4.97)	689 (4.97)
2	350 (4.73)	635[a] (4.38)		707 (4.99)	
4	352 (4.73)	626[a] (4.36)		690 (4.99)	

[a] Shoulder

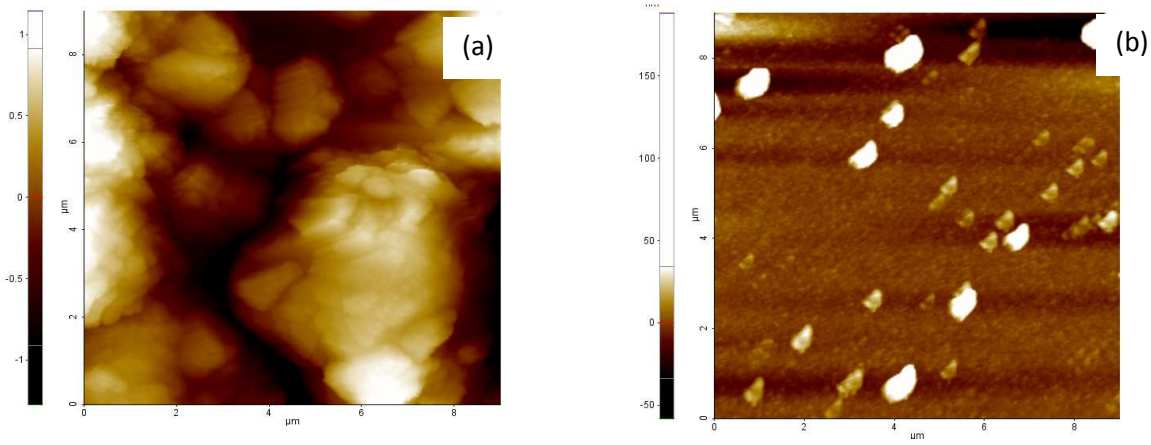

Figure 3. AFM topography of the films with **4.0**:1.0 (a) and **2.5**:1.0 (b) blend ratios

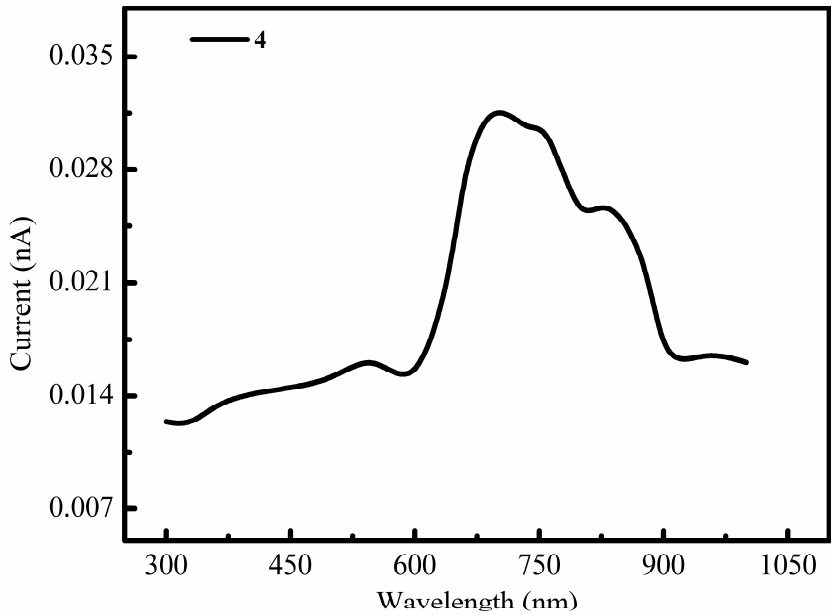

Figure 4. Variation of the photocurrent in **4** with the incident light wavelength.

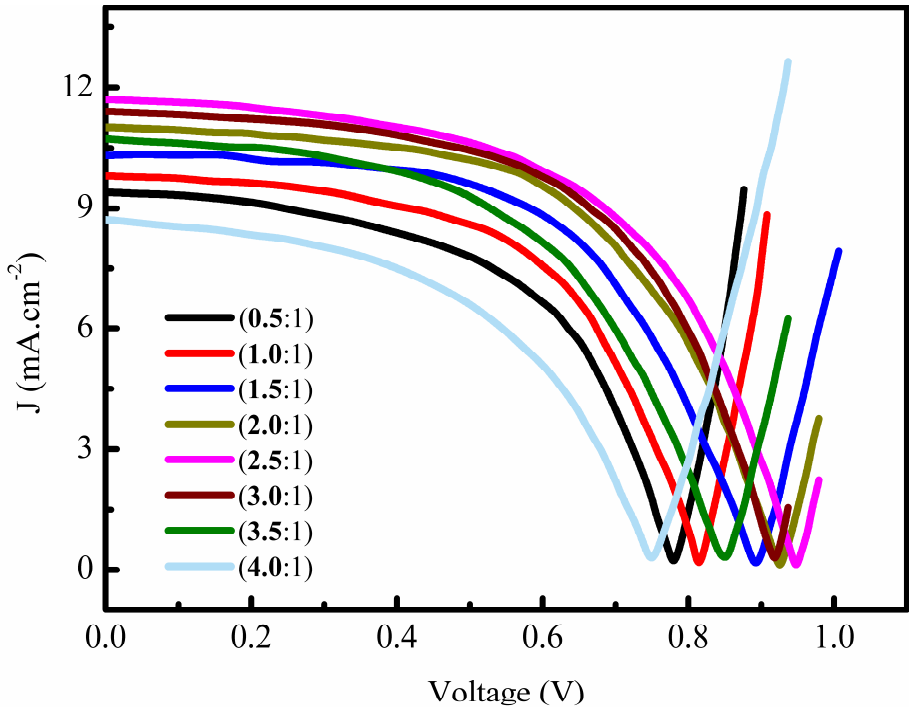

Figure 5. J-V characteristics of the **4** based device with various blend ratio

Table 2

Blend ratio dependence of the photovoltaic parameters for the investigated devices.

Blend Ratio	V_{OC} (V)	J_{SC} (mA cm^{-2})	V_m (V)	J_m (mA cm^{-2})	FF	η (%)
(**0.5:**1.0)	0.78	9.04	0.57	7.02	0.57	4.01
(**1.0:**1.0)	0.81	9.80	0.59	7.76	0.58	4.57
(**1.5:**1.0)	0.89	10.31	0.64	8.28	0.58	5.30
(**2.0:**1.0)	0.93	11.02	0.62	9.30	0.56	5.77
(**2.5:**1.0)	0.95	11.70	0.68	9.03	0.55	6.14
(**3.0:**1.0)	0.92	11.40	0.66	9.10	0.57	6.00
(**3.5:**1.0)	0.85	10.7 4	0.62	7.84	0.53	4.84
(**4.0:**1.0)	0.75	8.73	0.51	6.51	0.51	3.32

SUPPLEMENTARY INFORMATION

Unsymmetrical zinc phthalocyanines containing thiophene and amine groups as donor for bulk heterojunction solar cells

Gülnur KESER KARAOĞLAN[a,*], Öznur DÜLGER KUTLU[a], Ahmet ALTINDAL[b]

[a]Department of Chemistry, Yıldız Technical University, İstanbul-Turkey

[b]Department of Physics, Yıldız Technical University, İstanbul, Turkey

* Corresponding author. Fax: +90 264 295 74 26. E-mail address: gkeser@yildiz.edu.tr

1. Materials and equipment

[2(3),9(10),16(17),23(24)-Tetra-nitro-phthtalocyaninatozinc(II)] (**1**) and [2(3),9(10),16(17), 23(24)-Tetra-amino-phthtalocyaninatozinc(II)] (**2**) was synthesized according to the literature [26]. Di-3-thienyl ketone (**3**) was used as supplied commercially. *p*-Toluenesulfonic acid monohydrate was purchased from Sigma-Aldrich. Electronic spectra were recorded on an Agilent 8453 UV/Vis spectrophotometer. FT-IR spectra were recorded on a Perkin Elmer Spectrum One. ^{1}H NMR spectra were recorded in $CDCl_3$ and DMSO-d_6 solutions on a Varian 500 MHz spectrometer. Mass spectra were determined by a Bruker microflex LT MALDI-TOF MS. Electrothermal Gallenkamp apparatus was used for observing melting points of complexes.

2. Synthesis

2.1. 2(3),9(10),16(17),23(24)-Tetranitrophthtalocyaninatozinc(II) (1)

A mixture of compound 4-nitrophthalonitrile (600 mg, 3.466 mmol), anhydrous Zn $(CH_3COO)_2$ (159.72 mg, 0.866 mmol) and a catalytic amount of DBU in dry DMF (1 mL) was heated at 178 ^{o}C with stirring under argon atmosphere for 24 h. After cooling to room temperature, the reaction mixture was precipitated by adding methanol. The product was separated by filtration as a dark green solid. The precipitate was washed several times with methanol and ethanol to remove the unreacted starting materials and dried in vacuo. This compound is soluble in THF, DMF, DMSO and 1,4-dioxane. Yield: 505 mg (77%); m.p. > 200 $^{\circ}$C. FT-IR (ν_{max}/cm^{-1}): 3090 (Ar-H), 1518, 1324 (-NO_2), 1485, 1134, 1069, 1038, 904, 844,754,725; ^{1}H-NMR ($CDCl_3$) δ, ppm: 7.48-9.17 (12H, m, Ar- H); UV-Vis (THF): λmax(nm) (log ε) 689 (4.97), 679 (4.97), 639

(4.62), 617 (4.55), 350 (4.73); Anal. Calc. for $C_{32}H_{12}N_{12}O_8Zn$ (756.019 g mol^{-1}): C, 50.71; H, 1.60; N, 22.18; Found: C, 50.75; H, 1.66; N 21.91%; MS (MALDI-TOF): m/z (100%) 757.002 $[M+H]^+$.

2.2. 2(3),9(10),16(17),23(24)-Tetraaminophthtalocyaninatozinc(II) (2)

The compound **2** was obtained by reduction of **1**. A mixture of **1** (420 mg, 0.55 mmol), hydrazine hydrate (120 mL), and catalytic amount of 10% Pd/C was refluxed in dry 1,4-dioxane (70 mL) under argon atmosphere for 72 h. The cooled reaction mixture was quickly suction filtered. The residue that had been collected on the filter was discarded, and the filtrate was evaporated to dryness gently under vacuum in rotary evaporator and washed with cold water. After being dried in vacuum, the crude green product was obtained. Compound **2** is fairly soluble in $CHCl_3$, THF, DMF and DMSO. Yield: 0.1806 g (51%); m.p. > 200 $^{\circ}$C. FT-IR (ν_{max}/cm^{-1}): 3333, 3214, 1603 (NH_2), 3063 (Ar-H), 1493, 1456 (Ar C=C), 1253, 1091, 1045, 938, 826, 747; ^{1}H-NMR ($CDCl_3$) δ, ppm: 6.40-8.49 (12H, m, Ar-H), 4.2 (8H, s, -NH_2); UV-Vis (THF): λmax(nm) (log ε) 707 (4.99), 635 (4.38), 350 (4.73); Anal. Calc. for $C_{32}H_{20}N_{12}Zn$ (636.122 g mol^{-1}): C, 60.25; H, 3.16; N, 26.35; Found: C, 60.32; H, 3.19; N, 26.40. MS (MALDI-TOF): m/z (100%) 637.694 $[M+H]^+$.

2.3. [2(3),9(10)-Diamino-16(17),23(24)-bis(1,1-di(thiophen-2-yl)methanimino)phthalocyaninatozinc(II)] (4)

Di-2-thienyl methanone (**3**) (0.03 g, 0.156 mmol), [2(3),9(10),16(17),23(24)-tetra-amino-phthtalocyaninatozinc(II)] (**2**) (0.05 g, 0.078 mmol) and catalytic amount of *p*-toluenesulfonic acid monohydrate (*p*-TsOH·H_2O) as catalyst in dry DMF (5 mL) were stirred under inert atmosphere for 48 h at 160 ^{o}C. After the reaction mixture was left to cool into the room temperature, the solvent was evaporated under vacuum and then washed water, methanol, ethanol and *n*-hexane. After drying the crude product purification of this novel compound was

succeeded by column chromatography (TLC) using THF as an eluent. Yield: 0.072 g (45%); m.p.> 300 °C. FT-IR (ν_{max}/cm^{-1}): 3343, 3231, 1609 (-NH_2), 3064 (Ar–H), 1679 (-N=C), 1563, 1489 (Ar C=C), 1396, 1339, 1132, 1089, 951, 833, 814, 744. UV–Vis (THF): λmax(nm) (log ε) 690 (4.99), 626 (4.36), 352 (4.73); ^{1}H-NMR (DMSO-d_6) δ, ppm: 9.06–6.99 (24 H, m, Ar–H), 4.38 (4H, s, -NH_2). Anal. Calc. for $C_{50}H_{28}N_{12}S_4Zn$ (988.07 $gmol^{-1}$): C, 60.63; H, 2.85; N, 16.97; Found: C, 60.68; H, 2.79; N, 16.91. MS (MALDI-TOF): m/z (100%) 687.437 [M-2NH_2 – $C_9H_6NS_2$-C_4H_3S+2H]$^+$, 1013.27 [M+Na+2H]$^+$.

3. Production of bulk heterojunction devices and their characterizations

Devices were fabricated using fluorine doped tin oxide (FTO) coated glass substrates by using **4** and [6,6]-phenyl-C61-butyric acid methyl ester (PCBM) as donor and acceptor, respectively. The PCBM was purchased by Sigma Aldrich and used without any purification. For solar cell fabrication, the FTO coated glass substrates were thoroughly cleaned with a mixed solution of deionized water, acetone, and 2-propanol (volume rations of 1:1:1) under sonication for 40 min., and finally dried in flowing of dry nitrogen gas. After standard cleaning and UV treatment of FTO substrates, 30 nm hole injection layer of poly(3,4- ethylenedioxythiophene): poly(styrenesulfonate) (PEDOT:PSS) was spin coated followed by heat treatment at 110 ºC for 15 min. The reason for thermal annealing of the device at 110 °C is to ensure removal of the residual solvent in the films. According to present literature, although photo voltaic conversion efficiency (PCE) of up to 2.7% could be achieved by using tetrahydrofuran as solvent, PCEs close to 5% were only achieved using chlorinated solvent additives [27]. More recently, an oligomer based device from 2-methyltetrahydrofuran as processing solvent exhibiting PCEs of up to 5% was reported by Bazan et al. [28] Peng et al. [29] and Chu et al. [30] have been used toluene and *o*-xylene as solvent to prepare efficient devices with PCEs in the range of 5–7%. It is evident from all these studies that solvent used has a profound impact on the BHJ solar cell performance. As the solvent, we used dimethyl formamide (DMF) with a concentration of 1.2 ×

10^{-3} M for both PCBM and **4**. Interdigital micro array (IMA) of gold electrodes with 25 finger pairs having 50 μm width and space was used for both conductivity and photo current measurements. A homemade stainless steel chamber with a quartz window was used for photo current measurements. During photo current measurements, the films were illuminated by a 150 W Xenon lamp through a monochromator by varying the wavelength of the incident light from 300 to 1000 nm. Conductivity of the PEDOT:PSS film was obtained from the slope of the measured current–voltage (I-V) characteristics by using following equation;

$$\sigma = S\frac{d}{(2n-1)\ell.h} \qquad (1)$$

where, S is the slope of the I-V characteristic, d is distance between the finger pair, n is number of the finger pair, ℓ is overlap length of the electrodes and h is thickness of the electrodes.

In order to investigate the effect of the blend ratio, several BHJ devices were fabricated with various blend ratios between 0.5 and 4. Thin films of the active layer with nearly identical thicknesses were deposited on the hole injection layer of PEDOT:PSS by spin coating method. The active area of the devices was kept constant at 1.5×10^{-1} cm^2 in order to avoid the active area effect on device performance and the understanding of the physical effects involved. After the thermal treatment at 110 $^{\circ}$C for 15 min, a 300 nm thick aluminum cathode was thermally evaporated on the active layer through a shadow mask at 10^{-6} Torr. Ellipsometric technique was used to determine the thickness of the active layer. Ellipsometric measurements indicate that the thickness of the films varies between 110 and 115 nm. Photovoltaic characterizations of FTO/PEDOT:PSS/**4**:PCBM blend/Al structure with different **4**: PCBM ratio were carried out by means of current density (J)-voltage (V) measurements using a Keithley 2400 sourcemeter under AM 1.5 illumination conditions. In order to clarify the effect of the surface morphology of the blend film on the photovoltaic performance the surface morphology of the blend film were analyzed by atomic force microscopy technique. The AFM image analysis was carried out

using commercial XEP and XEI software procedures to determine the surface roughness characterized by the Root–Mean– Square (RMS) parameter.

MALDI TOF MS

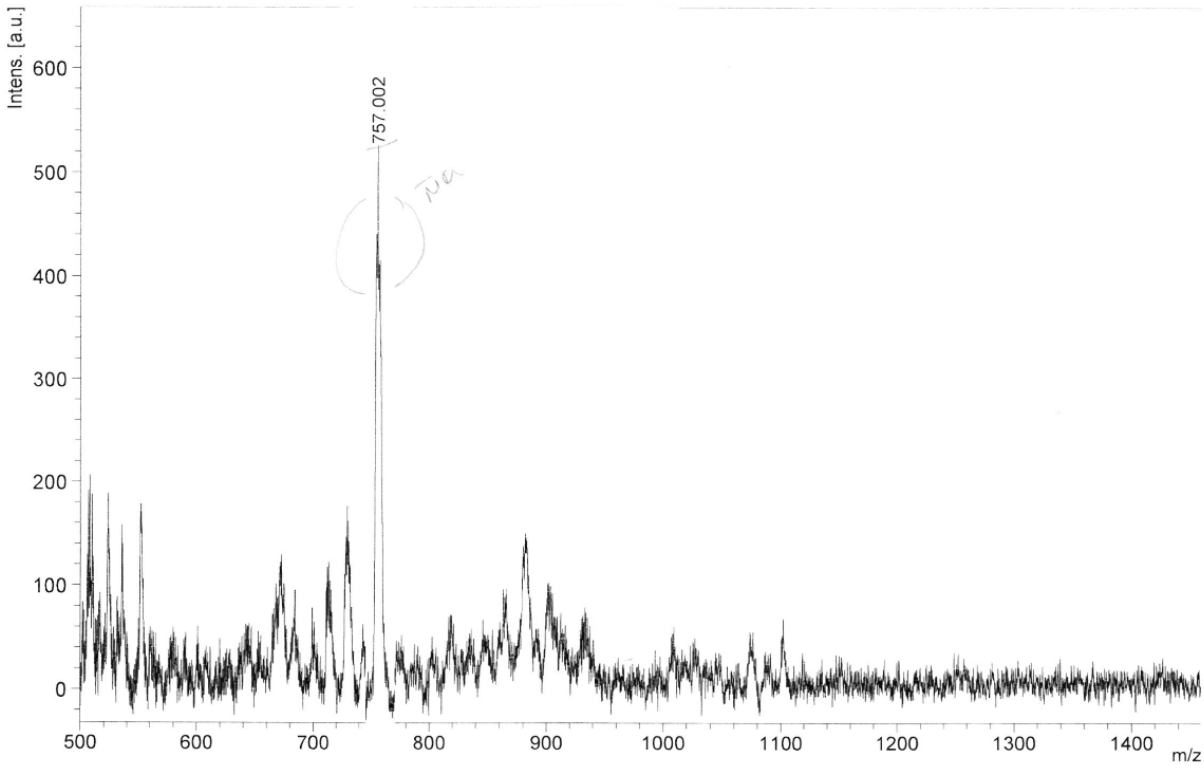

Figure S1. MS (MALDI-TOF) spectrum of compound **1**

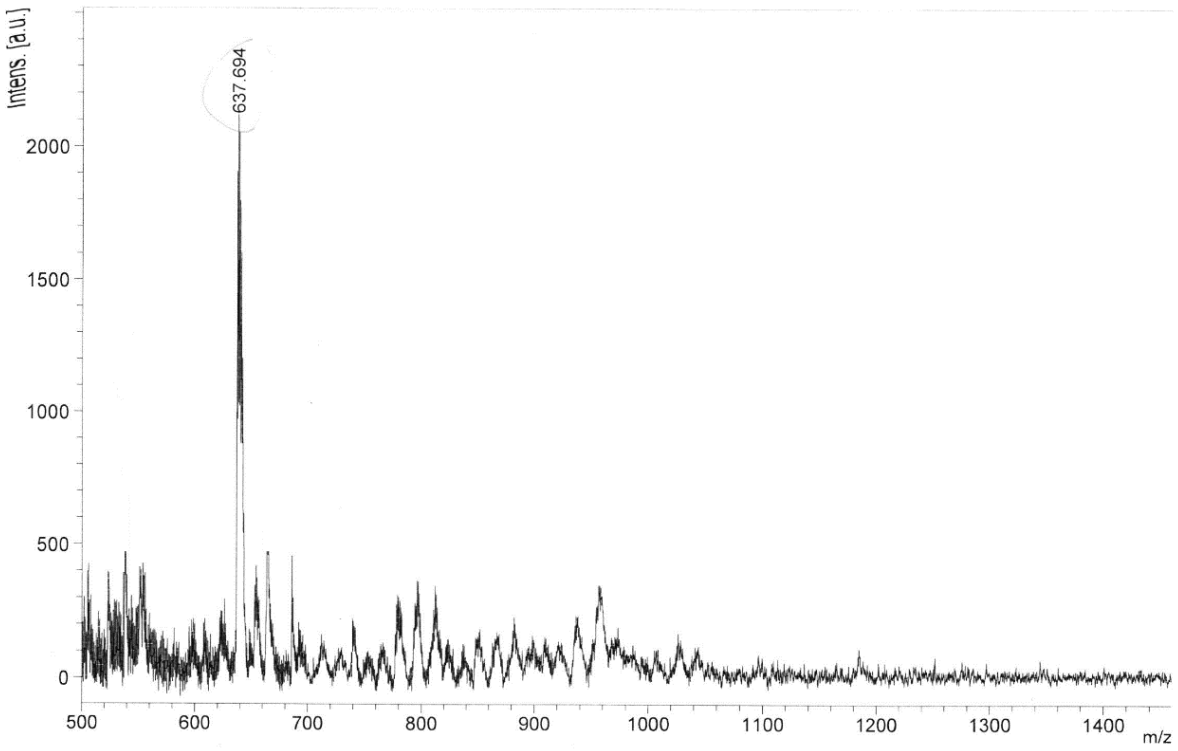

Figure S2. MS (MALDI-TOF) spectrum of compound **2**

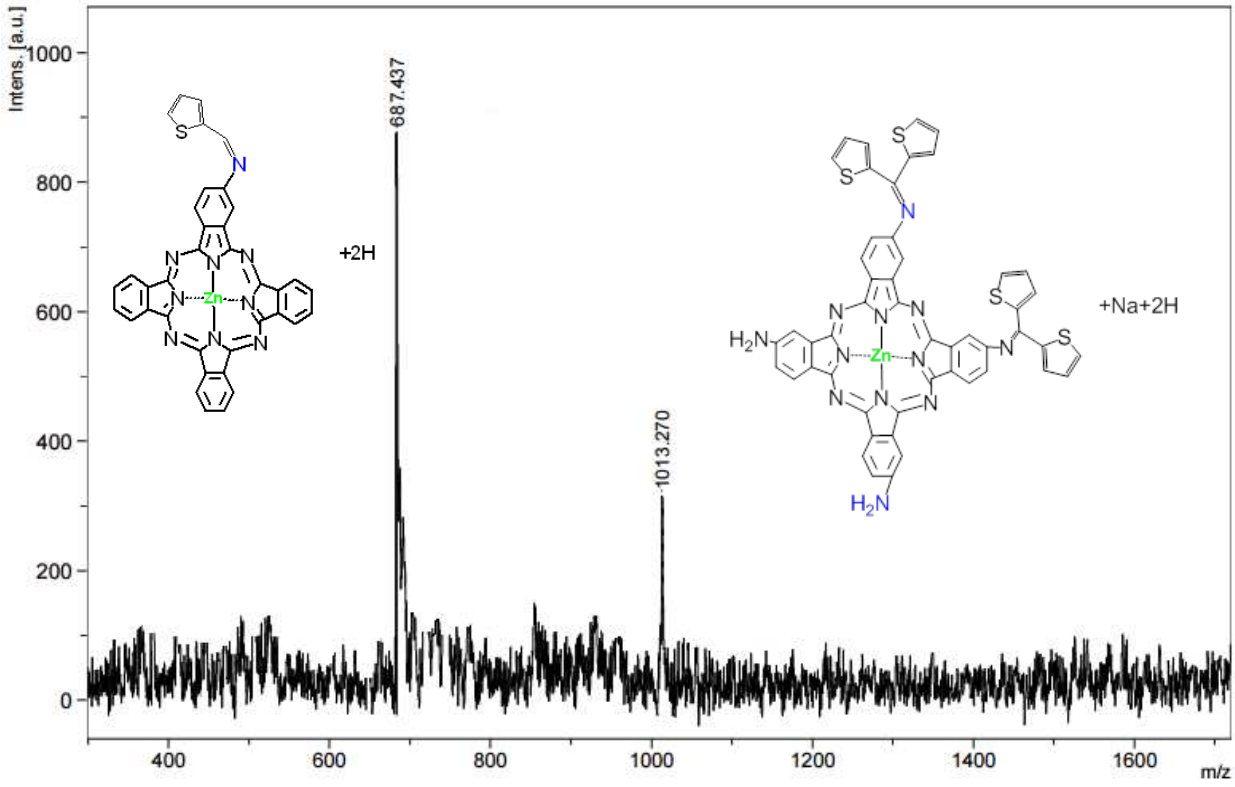

Figure S3. MS (MALDI-TOF) spectrum of compound **4**

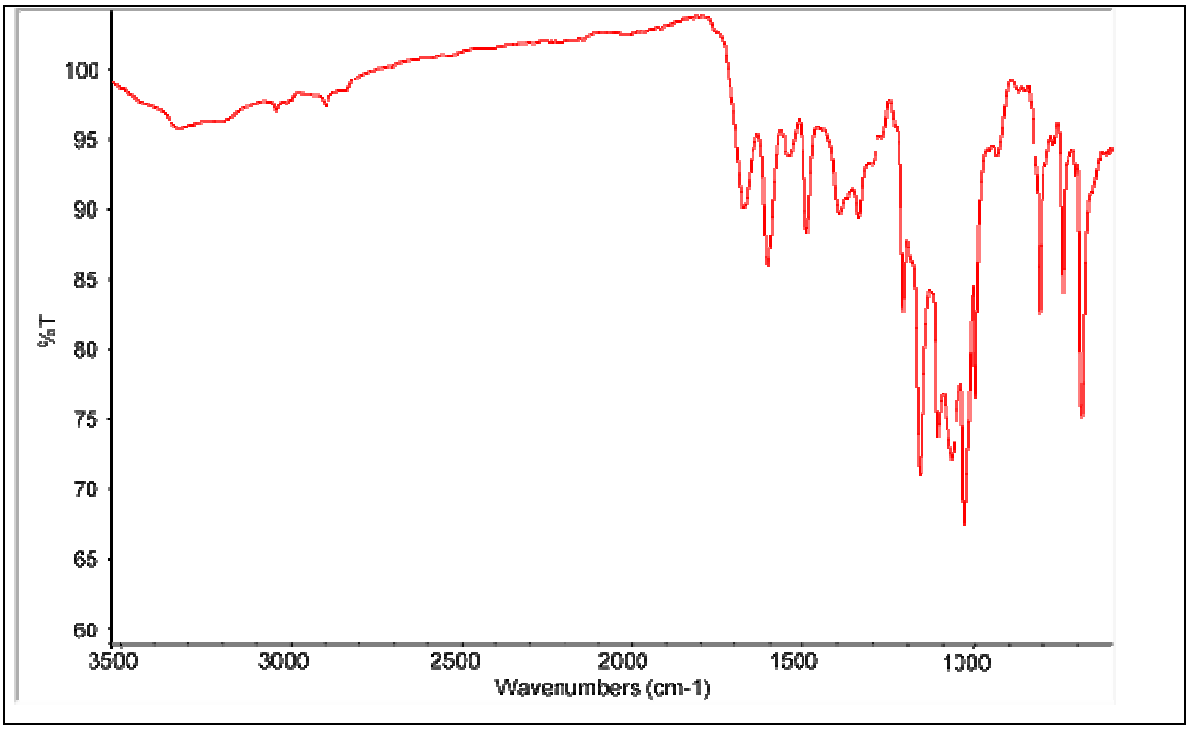

Figure S4. FT-IR spectrum of compound **4**